

# MR Elastography Analysis of Glioma Stiffness and *IDH1*-Mutation Status

K.M. Pepin, K.P. McGee, A. Arani, D.S. Lake, K.J. Glaser, A. Manduca, I.F. Parney, R.L. Ehman, and J. Huston III



## ABSTRACT

**BACKGROUND AND PURPOSE:** Our aim was to noninvasively evaluate gliomas with MR elastography to characterize the relationship of tumor stiffness with tumor grade and mutations in the *isocitrate dehydrogenase 1 (IDH1)* gene.

**MATERIALS AND METHODS:** Tumor stiffness properties were prospectively quantified in 18 patients (mean age, 42 years; 6 women) with histologically proved gliomas using MR elastography from 2014 to 2016. Images were acquired on a 3T MR imaging unit with a vibration frequency of 60 Hz. Tumor stiffness was compared with unaffected contralateral white matter, across tumor grade, and by *IDH1*-mutation status. The performance of the use of tumor stiffness to predict tumor grade and *IDH1* mutation was evaluated with the Wilcoxon rank sum, 1-way ANOVA, and Tukey-Kramer tests.

**RESULTS:** Gliomas were softer than healthy brain parenchyma, 2.2 kPa compared with 3.3 kPa ( $P < .001$ ), with grade IV tumors softer than grade II. Tumors with an *IDH1* mutation were significantly stiffer than those with wild type *IDH1*, 2.5 kPa versus 1.6 kPa, respectively ( $P = .007$ ).

**CONCLUSIONS:** MR elastography demonstrated that not only were gliomas softer than normal brain but the degree of softening was directly correlated with tumor grade and *IDH1*-mutation status. Noninvasive determination of tumor grade and *IDH1* mutation may result in improved stratification of patients for different treatment options and the evaluation of novel therapeutics. This work reports on the emerging field of “mechanogenomics”: the identification of genetic features such as *IDH1* mutation using intrinsic biomechanical information.

**ABBREVIATIONS:** GBM = glioblastoma; ECM = extracellular matrix;  $|G^*|$  = magnitude of the complex shear modulus; *IDH1* = *isocitrate dehydrogenase 1*; MRE = MR elastography

While gliomas are rare compared with other cancers, they have a high mortality rate. Despite improvement in 5-year survival rates of many cancers, outcomes for brain tumors have remained relatively unchanged during the past 30 years, improving <2%.<sup>1</sup> Median survival is 12–15 months for glioblastomas (GBMs) and 2–5 years for lower grade gliomas. As our understanding of cancer biology, genetics, and treatment resistance mechanisms improves, the ability to stratify patients early with predictive biomarkers will be critical in the development of new

therapies and the evaluation of treatment responses.<sup>2</sup> Gliomas are histopathologically typed and graded as outlined with the World Health Organization criteria, which provide important prognostic information as well as potential guidance on the clinical treatment of the tumor.<sup>3</sup> The World Health Organization classification was updated in 2016 to include molecular markers, which have important implications for patient outcome and may be critical information in the selection of a treatment strategy. Recent effort in the area of radiogenomics has explored the potential of using MR imaging phenotypes to noninvasively determine tumor genotypes, including the detection of 3 common genomic alterations in gliomas.<sup>4</sup> Mutations in the gene responsible for encoding a metabolic enzyme called *isocitrate dehydrogenase 1 (IDH1)* frequently occur in low-grade gliomas, exhibiting different genetic and epigenetic etiology compared with *IDH1* wild type gliomas, and are considered a distinct disease entity with a poorer prognosis, independent of tumor grade.<sup>5,6</sup>

While only 6% of GBMs have mutations in *IDH1*, it is hypothesized that these tumors have evolved from lower grade gliomas, while low-grade gliomas that lack a mutation in *IDH1* could be

Received May 30, 2017; accepted after revision August 13.

From the Mayo Graduate School (K.M.P.) and Departments of Radiology (K.P.M., A.A., D.S.L., K.J.G., A.M., R.L.E., J.H.) and Neurosurgery (I.F.P.), Mayo Clinic College of Medicine, Rochester, Minnesota.

This work was supported, in part, by grants from the National Institutes of Health RO1 EB001981 and the Center for Individualizing Medicine, Imaging Biomarker Discovery Program, Mayo Clinic.

Please address correspondence to John Huston III, MD, Mayo Clinic College of Medicine, 200 First St SW, No. W4, Rochester, MN 55905; e-mail: jhuston@mayo.edu

Indicates open access to non-subscribers at www.ajnr.org

<http://dx.doi.org/10.3174/ajnr.A5415>

considered “preglioblastomas.”<sup>5,7</sup> *IDH1* mutations may also be predictive of therapeutic outcome from specific treatments, such as increased radiosensitivity in vitro and differentiating patients who benefit from alkylating agent chemotherapy in combination with radiation therapy.<sup>8,9</sup> Recent effort has investigated noninvasive biomarkers to identify *IDH1*-mutant tumors in humans, including MR spectroscopy, using the association between mutations in *IDH1* and 2-hydroxyglutarate in the tumor.<sup>10</sup> However, challenges related to long scan times, complex data processing, and low spectral resolution have limited clinical applications.<sup>11</sup>

Tumors are characterized by altered tissue- and cellular-level mechanics, and the stiffness of the extracellular matrix (ECM) in gliomas may be associated with a mutation in *IDH1*.<sup>12,13</sup> A recent study by Miroshnikova et al<sup>13</sup> demonstrated an overall correlation between tumor grade and *IDH1* mutational status with the ECM stiffness of human glioma brain biopsies. Using stiffness measurements from an atomic force microscope, they demonstrated increased ECM stiffness with tumor grade: The ECM from GBMs was stiffer than the ECM from lower grade gliomas. Additionally, the ECM of gliomas with a mutation in *IDH1* was softer than the ECM of wild type *IDH1* gliomas, regardless of histologic grade. These results demonstrate a microscopic mechanical correlation between ECM stiffness and tumor genotype. Additional work is needed to determine whether this finding correlates to macroscopic mechanical properties of gliomas.

MR elastography (MRE) is a technique used to noninvasively quantify the mechanical properties of tissue.<sup>14–16</sup> Previous studies have demonstrated the feasibility of using MRE to evaluate the viscoelastic properties of brain tumors, including gliomas, in which brain tumors were mainly softer than normal brain and benign variants; however, some tumors are stiffer than normal brain,<sup>17</sup> and GBMs were the softest brain tumors compared with meningiomas, vestibular schwannomas, and metastases.<sup>18,19</sup> Additional work demonstrated that the viscoelastic properties of GBMs were dependent on composition (eg, necrosis or cystic cavities) and that the mechanical properties were heterogeneous with both stiff and soft regions.<sup>17,20</sup> Recent work investigated the stiffness of 4 common brain tumors and stated that MRE may reflect the collagenous content of tumors.<sup>19</sup>

The purpose of this study was to noninvasively evaluate gliomas with MRE to characterize the relationship of tumor stiffness with tumor grade and mutations in the *IDH1* gene. We hypothesize that glioma stiffness will vary across tumor grade and that gliomas with an *IDH1* mutation will exhibit different mechanical properties than *IDH1* wild type gliomas.

## MATERIALS AND METHODS

### Patient Recruitment

This prospective study was approved by our institutional review board, and informed written consent was obtained from each subject. Inclusion criteria for the study consisted of subjects older than 18 years of age with biopsy-confirmed gliomas and a minimum tumor diameter of 2 cm. Subjects with contraindications to MR imaging (cardiac pacemaker, implanted metallic object, or claustrophobia) and lesions with extensive necrosis were excluded. Eighteen patients (mean age, 44 years; range, 25–68 for men,  $n = 12$ ; and mean age, 40 years; range, 28–40 for women,

$n = 6$ ) with a presumed or previous needle biopsy–diagnosed glioma scheduled for surgical resection were recruited for an MRE examination before tumor resection from April 2014 to December 2016. Diagnosis was confirmed following the operation by an experienced pathologist as part of clinical standard of care and included determination of tumor grade, histologic subtype, the presence of the 1p/19q codeletion, and *IDH1-R132H* mutations.

### MR Image Acquisition

Preoperative imaging was performed with a 3T MR imaging scanner (Signa Excite; GE Healthcare, Milwaukee, Wisconsin). The MR imaging protocol for each subject included an anatomic T1-weighted inversion recovery echo-spoiled gradient-echo acquisition with the following parameters: TR/TE = 6.3/2.8 ms; TI = 400 ms; flip angle = 11°; 256 × 256 acquisition matrix; FOV = 27 cm; section thickness = 1.2 mm; 200 sagittal sections; bandwidth = 31.25 kHz; parallel imaging acceleration factor = 1.75. MRE imaging used a modified single-shot, flow-compensated, spin-echo EPI pulse sequence.<sup>21,22</sup>

### MR Elastography Image Acquisition

Low-amplitude mechanical vibrations in the form of shear waves were introduced into the brain at a frequency of 60 Hz as previously described.<sup>23</sup> A custom-built soft, pillowlike passive driver was positioned beneath the subject’s head in a standard 8-channel receive-only MR imaging head coil (Fig 1). A long flexible tube connected the passive driver to the active component located outside the scan room, which comprised a waveform generator, an amplifier, and an acoustic speaker. The resulting shear wave motion was imaged with the spin-echo EPI MRE pulse sequence by synchronizing motion-encoding gradients to the applied mechanical vibrations. The imaging parameters included the following: TR/TE = 3600/62 ms; 72 × 72 acquisition matrix reconstructed to 80 × 80; FOV = 24 cm; section thickness = 3 mm; 48 contiguous axial sections; bandwidth = 250 kHz; parallel imaging acceleration factor = 3; motion-encoding in the positive and negative x, y, and z directions; and 8 phase offsets sampled during 1 period of motion at 60 Hz. The MRE acquisition time was <7 minutes.

### Image and Data Processing

Tissue viscoelastic shear properties were quantified from the measured displacement fields.<sup>14,24,25</sup> Assuming the tissue to be linear, isotropic, locally homogeneous, and viscoelastic, we quantified the complex shear modulus using previously described direct inversion methods (Fig 1).<sup>22,26–28</sup> Before direct inversion, several postprocessing steps were taken. First, the complex phase-difference images were calculated in the x, y, and z motion-encoding directions. Then, the curl of the input displacement field was calculated to reduce effects from the tissue boundaries and longitudinal wave propagation. A 2D low-pass filter was applied to reduce section-to-section phase discontinuities. A 3D direct inversion algorithm was used to calculate the complex shear modulus  $G^*$ .<sup>22</sup> Shear stiffness was reported as the magnitude of the complex shear modulus ( $|G^*|$ ). A tumor ROI was manually drawn on each imaging section from T1-maps registered to the MRE space using information from all available imaging

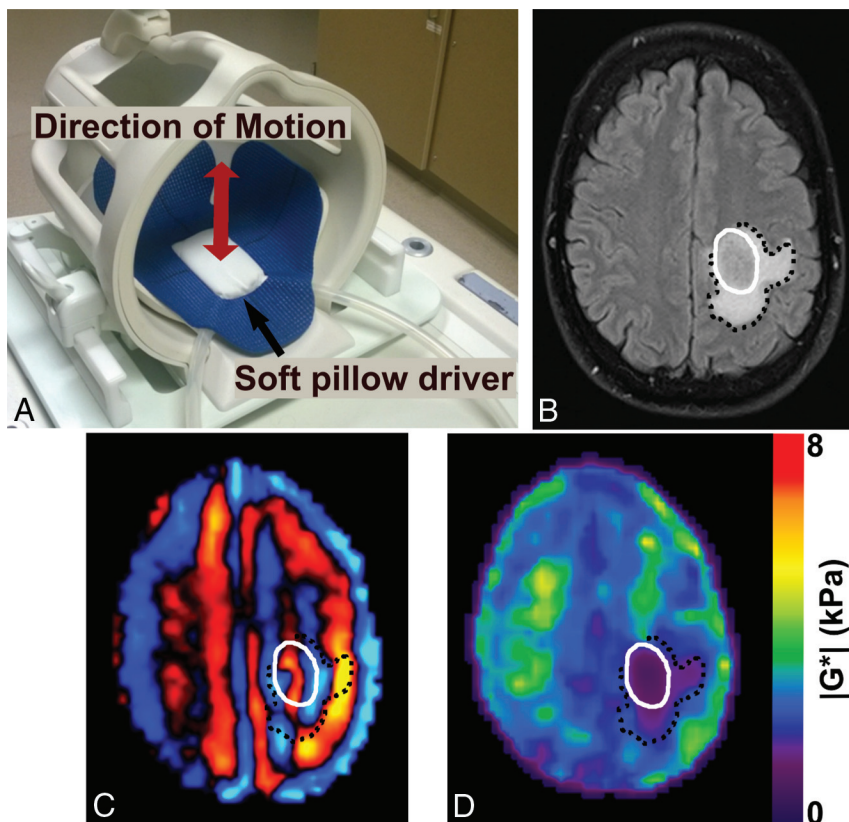


**FIG 1.** Brain MRE experimental setup and image processing. **A**, Brain MRE soft pillow driver placed within the 8-channel MR imaging head coil and positioned beneath the head to induce shear waves in the brain. **B**, Axial T2 FLAIR image of a glioblastoma, *IDH1* wild type (51-year-old man), with tumor denoted by a solid white line, and peritumoral edema, by a black dotted line. MRE shear wave image (**C**) and elastogram (**D**) or stiffness map display a soft tumor with a stiffness of 1.1 kPa in the tumor compared with 3.5 kPa in a size-matched region of unaffected white matter on the contralateral hemisphere.

sequences, including T1-, T2-, diffusion-, and contrast-enhanced T1-weighted images as previously described (research trainees, 1 year of experience under supervision of J.H., 26 years' experience).<sup>22</sup> Tumor stiffness was calculated as the median  $|G^*|$  of all voxels contained in the ROI volume and was compared with a size-matched ROI in the unaffected white matter on the contralateral hemisphere to serve as a control. Group results are reported as mean  $\pm$  SD (range).

Tumor volume was defined as the tumor ROI volume (cubic centimeter), calculated as the number of voxels contained in the ROI multiplied by the voxel volume. Contrast enhancement was assigned a label of nonenhancing, partially enhancing, or completely enhancing, determined from contrast-enhanced T1-weighted images obtained during a standard diagnostic MR imaging (J.H., 26 years' experience in neuroradiology).

### Statistical Analysis

For each tumor ROI volume, the mean difference in tumor shear stiffness and unaffected contralateral normal white matter was analyzed with the Wilcoxon rank sum test. The mean differences in mean shear stiffness of *IDH1*<sup>+</sup> and *IDH1*<sup>−</sup> tumors were analyzed with the Wilcoxon rank sum test. One-way ANOVA and Tukey-Kramer tests were used to compare the mean tumor shear stiffness between different tumor grades. A *P* value of  $< .05$  was

considered statistically significant. All calculations were performed with Matlab 2016a (MathWorks, Natick, Massachusetts) and R Core Team, 2015 (R Foundation for Statistical Computing, Vienna, Austria; <http://www.r-project.org>).

## RESULTS

### Patient Recruitment

MRE was performed on 18 patients. Following the operation, tumor grade was determined by clinical pathology and included 5 grade II, 7 grade III, and 6 grade IV tumors (Table). Twelve patients had tumors with a mutation in *IDH1-R132H*: 5/5 grade II, 5/7 grade III, and 2/6 grade IV tumors. Following the revision of the World Health Organization classification of gliomas in 2016, the 18 histopathology results were reclassified to reflect the new definitions.

### Shear Stiffness and Tumor Grade

The mean shear stiffness of all gliomas was  $2.2 \pm 0.7$  kPa (range, 1.1–3.8 kPa) compared with  $3.3 \pm 0.7$  kPa (range, 1.2–4.1 kPa) in the contralateral unaffected white matter. In all except 2 cases, the tumor tissues were softer than normal brain tissue ( $P < .001$ ). Tumor stiffness showed an inverse relationship with tumor grade: High-grade tumors were softer than lower grade tumors (Fig 2).

For grades II, III, and IV, tumor stiffness

was  $2.7 \pm 0.7$  kPa (range, 2.1–3.8 kPa),  $2.2 \pm 0.6$  kPa (range, 1.7–3.4 kPa), and  $1.7 \pm 0.5$  kPa (range, 1.3–2.1 kPa), respectively. Grade IV GBMs were significantly softer than grade II gliomas ( $P = .03$ ), but no statistically significant difference between grades II and III ( $P = .19$ ) or between grades III and IV ( $P = .23$ ) was observed. Additional correlations of tumor stiffness were investigated, including anatomic location, patient age, and tumor volume, but no significant trends were observed.

### Shear Stiffness and *IDH1* Mutations

Tumors with a mutation in *IDH1* ( $n = 12$ ) were significantly stiffer than wild type *IDH1* ( $n = 6$ ) tumors, with a shear stiffness of  $2.5 \pm 0.6$  kPa (range, 1.5–3.8 kPa) and  $1.6 \pm 0.3$  kPa (range, 1.1–1.9 kPa), respectively ( $P = .007$ , Fig 3). This observation was independent of tumor grade. There were 2 outliers, including a secondary GBM with a positive *IDH1* mutation and a shear stiffness of 1.5 kPa and a grade III infiltrating anaplastic glioma with a positive *IDH1* mutation and a shear modulus of 1.7 kPa. The MRE results from 2 grade III tumors are shown in Fig 4, to demonstrate the large stiffness heterogeneity between *IDH1* mutant and wild type tumors. While both were grade III gliomas, the mechanical properties were drastically different between the 2 tumors, with tumor stiffness equal to 3.3 kPa for the *IDH1* mutant tumor and 1.7 kPa for the *IDH1* wild type tumor.

## Patient and tumor characteristics

No.	Sex	Age (yr)	Tumor Size (cm <sup>3</sup> )	Location	Contrast Enhancement	IDH1 Mutated?	1p/19q Codeleted?	Histologic and Genetic Classification	Grade
1	F	36	16.8	Left parietal	None	Yes	Yes	Oligodendroglioma, IDH mutant and 1p19q codeleted	II
2	M	39	60.6	Right temporal	None	Yes	No	Diffuse astrocytoma, IDH mutant	II
3	M	34	14.7	Left frontal	Partial	Yes	No	Diffuse astrocytoma, IDH mutant	II
4	M	31	54.7	Right frontal	None	Yes	Yes	Oligodendroglioma, IDH mutant and 1p19q codeleted	II
5	M	65	4.1	Left frontal	None	Yes	Yes	Oligodendroglioma	II
6	M	31	37.5	Left frontal	None	Yes	Yes	Oligodendroglioma, IDH mutant and 1p19q codeleted	III
7	F	35	66.9	Right frontal	None	Yes	No	Diffuse astrocytoma, IDH mutant	III
8	F	37	71.0	Left temporal	Partial	Yes	No	Diffuse astrocytoma, IDH mutant	III
9	M	51	59.9	Left temporal	None	Yes	Yes	Oligodendroglioma, IDH mutant and 1p19q codeleted	III
10	F	60	117.0	Right frontal	Partial	Yes	No	Diffuse astrocytoma, IDH mutant	III
11	F	44	75.6	Right frontal	None	No	No	Diffuse astrocytoma, IDH wild type	III
12	M	33	38.9	Left frontal	Partial	No	No	Diffuse astrocytoma, IDH wild type	III
13	F	28	5.5	Left frontal	Partial	Yes	—	Glioblastoma	IV
14	M	25	98.3	Right frontal	Partial	Yes	—	Glioblastoma	IV
15	M	51	27.6	Left postcentral gyrus	Complete	No	—	Glioblastoma	IV
16	M	46	9.5	Left temporal	None	No	—	Glioblastoma	IV
17	M	68	7.3	Left frontal	Complete	No	—	Glioblastoma	IV
18	M	55	37.1	Right thalamus	Complete	No	—	Glioblastoma	IV

**Note:** — indicates not applicable.

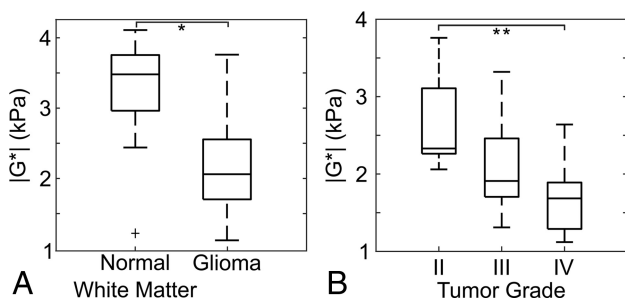


**FIG 2.** A, Gliomas are softer than normal brain tissue, compared with size-matched ROIs in the unaffected contralateral white matter (asterisk indicates  $P < .001$ ). An outlier is indicated by a plus sign, and whiskers on the boxplot indicate the 25th and 75th percentiles. B, Glioma stiffness decreases with increasing tumor grade (double asterisks indicate  $P < .05$ ).

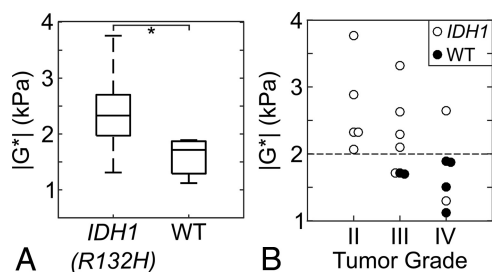


**FIG 3.** A, Comparison of the tumor stiffness ( $|G^*|$ ) between IDH1-R132H ( $n = 12$ ) and wild type (WT) gliomas ( $n = 6$ ). Gliomas with wild type IDH1 were significantly softer than gliomas with a mutation in IDH1-R132H (asterisk indicates  $P = .007$ ). The whiskers on the boxplot indicate the 25th and 75th percentiles. B, Tumor shear stiffness by tumor grade for all patients in this study including IDH1-R132H mutated tumors (white circles) and wild type IDH1 (WT, black circles). The horizontal dotted line at 2.0 kPa separates the IDH1-R132H mutated and wild type gliomas with a sensitivity and specificity of 83% and 100%. There is one secondary IDH1-mutated GBM with a low  $|G^*| = 1.5$  kPa, and it may be unique due to the secondary disease subtype.

## DISCUSSION

This study demonstrates that gliomas are softer than normal brain and that the stiffness of gliomas decreases with increasing tumor grade, consistent with previous MRE results of brain tumors. One

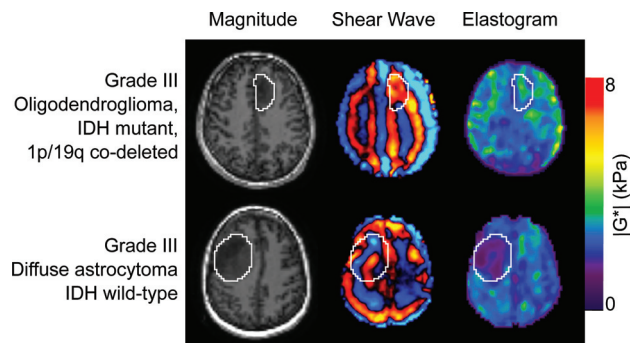


**FIG 4.** Stiffness heterogeneity of gliomas. Noncontrast, axial MRE magnitude images (left column), shear wave images (middle column), and elastograms (right column) for 2 patients with grade III gliomas. Images in the top row are from an oligodendroglioma with an IDH1-R132H mutation with  $|G^*| = 3.3$  kPa (a 31-year-old man), while the bottom row is from a diffuse astrocytoma with wild type IDH1 with  $|G^*| = 1.7$  kPa (a 44-year-old woman).

study reported that primary brain tumors have a uniform loss of dissipative behavior and that the tumor mechanical properties are altered with increasing malignancy.<sup>18</sup> Similarly, another study investigated the mechanical properties of GBMs using MRE and found that most GBMs were softer than normal brain.<sup>20</sup> In these studies, low-grade gliomas were not included and no statistical analysis was reported for the relationship between tumor mechanical properties and tumor grade or IDH1-mutation status. A recent study demonstrated good correlation between glioma stiffness measurements and surgical assessment.<sup>19</sup> The results of this study are consistent with the quantitative stiffness values of gliomas reported in the literature.

The results presented in this work suggest that glioma stiffness may be a biomarker of IDH1-mutation status, with softer tumors being indicative of a wild type IDH1, irrespective of tumor grade. IDH1 mutations in gliomas are associated with improved outcome.<sup>5</sup> The stiffness of the grade III gliomas with wild type IDH1 was more comparable with the stiffness of grade IV tumors than of the IDH1-mutated grade III tumors. One outlier was an IDH1-mutated GBM with a relatively low stiffness (1.5 kPa compared



with a mean of 2.5 kPa for *IDH*-mutated gliomas). This tumor was a secondary GBM; 76% of secondary GBMs are *IDH1*-mutated compared with 6% of primary GBMs.<sup>5,6</sup> The considerable softness of this GBM may be from previous radiation therapy. Further investigation is needed to understand the heterogeneity in glioma stiffness between primary and secondary malignancies for all tumor grades and different histologic subtypes. These data provide the evidence to support the concept of “mechanogenomics”—the identification of genetic features such as *IDH1* mutation using intrinsic biomechanical information and MRE-derived shear stiffness—possibly being used as a biomarker to both identify and spatially resolve genetically induced alterations of tissue biomechanical properties.

This study found an inverse relationship between tumor stiffness, in which GBMs were softer than lower grade tumors and gliomas with wild type *IDH1* were softer than those with mutated *IDH1*, regardless of tumor grade. This is opposite of the relationship found in the recent study by Miroshnikova et al<sup>13</sup> of ECM stiffness in gliomas, in which the ECM of gliomas with an *IDH1* mutation was associated with a softer ECM, independent of histologic grade. Macroscopic tumor stiffness comprises >1 constituent part, and in that study, ECM stiffness was not correlated with the levels or distribution of type I collagen, vasculature, or cellularity. Additional factors that may affect macroscopic tumor stiffness include cellularity, increased vessel density, and interstitial fluid pressure.<sup>29,30</sup> Each of these factors may contribute to the overall tumor stiffness and potentially explain the opposite relationship of whole-tumor stiffness with tumor grade and *IDH1*-mutation status observed in this study. While the opposite trends were observed in this study, the same correlations were found in which stiffness was correlated with tumor grade and *IDH1* mutations, irrespective of tumor grade. Further work is needed to understand the relationship between the microscopic ECM stiffness and the macroscopic whole-tumor stiffness in gliomas.

The mechanisms behind these mechanogenomic differences are not well-understood and therefore require further investigation to determine the diagnostic accuracy of this technique and to investigate the relationship between tumor mechanical properties and progression-free survival and overall survival. Additionally, the role of other common somatic driver mutations, including the codeletion of the 1p and 19q chromosomal arms, methylguanine methyltransferase methylation status, and *TERT* promotor mutations need to be investigated. In the case of low-grade gliomas, there is an important need for a noninvasive technique capable of detecting malignant transformation to a higher grade. The serial assessment of tumor mechanical properties using MRE may help identify these events before imaging changes on standard anatomic MR imaging are seen. Previous results suggesting the completeness of nonenhancing tumor resection are an important prognostic factor in *IDH1*-mutant tumors, and a priori knowledge of *IDH1* status may help guide the extent of planned resection.<sup>31</sup> The potential of mechanogenomics with MRE to reliably and prospectively identify *IDH1* mutation preoperatively may have a large impact on surgical planning and postoperative patient management.

There are several limitations in this pilot study, including sample size and representation of lower grade tumors. The inclusion

criteria for this study required a minimum tumor diameter of 2 cm. Improvement in the MRE acquisition and data processing could allow the quantification of mechanical properties in smaller tumors. Imaging plays an invaluable role in the treatment and monitoring of gliomas, but there is room for improvement. Common critiques of imaging techniques are low specificity and lack of histologic correlation. For instance, in the area of therapeutic response, the development of new targeted chemotherapy and radiation therapies may result in complicated imaging changes (either pseudoprogression or pseudoresponse), which are not adequately assessed with morphologic or anatomic imaging techniques. While our understanding of *IDH1* mutations and glioma biology has increased dramatically during the past few years, the optimal strategies for therapeutic interventions remain unclear. The ability to noninvasively detect this mutation may have important implications for stratifying patients for treatment and monitoring of response. Future work is needed to confirm these results and investigate additional tumor genotypes with prognostic and therapeutic significance for gliomas, including the 1p19q codeletion and methylguanine methyltransferase methylation status, as well as stiffness differences with histopathologic subtype.

## CONCLUSIONS

Our study confirms that gliomas of all grades are softer than normal brain tissue and that tumor stiffness decreases with increasing tumor grade. In addition, gliomas with a mutation in *IDH1* are stiffer than wild type *IDH1* gliomas. The quantitative analysis of brain tumor mechanical properties may aid in the initial clinical assessment, surgical management, and postoperative monitoring of gliomas.

## ACKNOWLEDGMENTS

The authors would like to thank Nikoo Fattahi, MD, Mona El Sheikh, MD, and Jann Sarkaria, MD, for their technical contributions. We would also like to thank Sonia Watson and Andrea Moran for their assistance in editing the manuscript.

Disclosures: Kiaran P. McGee—UNRELATED: Royalties: Resoundant; Stock/Stock Options: Resoundant. Kevin J. Glaser—UNRELATED: Patents (Planned, Pending or Issued): MR Elastography Technology, Comments: Mayo Clinic and Kevin J. Glaser have patents covering MR elastography technology\*; Royalties: MR Elastography Technology, Comments: Mayo Clinic and Kevin J. Glaser receive royalties from the licensing of MR elastography and technology; Stock/Stock Options: Resoundant, Comments: Kevin J. Glaser owns stock in Resoundant, a company owned by Mayo Clinic. Armando Manduca—UNRELATED: Royalties: Resoundant, Comments: Mayo Clinic and I receive some royalties for general activities in the field of MR elastography, though nothing specific to this work; Stock/Stock Options: Resoundant, Comments: I own some stock in Resoundant, a company that works in the general area of MR elastography. Richard L. Ehman—RELATED: Grant: National Institutes of Health EB001981\*; UNRELATED: Board Membership: Resoundant, Comments: uncompensated\*; Grants/Grants Pending: Resoundant\*; Patents (Planned, Pending or Issued): intellectual property related to MR elastography\*; Royalties: Mayo Clinic; Stock/Stock Options: Resoundant\*; Travel/Accommodations/Meeting Expenses Unrelated to Activities Listed: Radiological Society of North America, Resoundant, Bristol-Myers Squibb.\* John Huston—UNRELATED: Royalties: Mayo Clinic, Comments: for MR elastography intellectual property; Stock/Stock Options: Resoundant.\*Money paid to the institution.

## REFERENCES

1. Australian Institute of Health and Welfare. *Cancer in Australia: An Overview 2014*. Cancer Series No. 90. Cat. No. CAN 88. Canberra: Australian Institute of Health and Welfare; 2014
2. Miles K. Can imaging help improve the survival of cancer patients? *Cancer Imaging* 2011;1:Spec No A:S86–92 CrossRef Medline

3. Louis DN, Perry A, Reifenberger G, et al. **The 2016 World Health Organization Classification of Tumors of the Central Nervous System: a summary.** *Acta Neuropathol* 2016;131:803–20 [CrossRef Medline](#)
4. Smits M, van den Bent MJ. **Imaging correlates of adult glioma genotypes.** *Radiology* 2017;284:316–31 [CrossRef Medline](#)
5. Yan H, Parsons DW, Jin G, et al. **IDH1 and IDH2 mutations in gliomas.** *N Engl J Med* 2009;360:765–73 [CrossRef Medline](#)
6. Labussiere M, Sanson M, Idhah A, et al. **IDH1 gene mutations: a new paradigm in glioma prognosis and therapy?** *Oncologist* 2010;15:196–99 [CrossRef Medline](#)
7. Gorovets D, Kannan K, Shen R, et al. **IDH mutation and neuroglial developmental features define clinically distinct subclasses of lower grade diffuse astrocytic glioma.** *Clin Cancer Res* 2012;18:2490–501 [CrossRef Medline](#)
8. Li S, Chou AP, Chen W, et al. **Overexpression of isocitrate dehydrogenase mutant proteins renders glioma cells more sensitive to radiation.** *Neuro Oncol* 2013;15:57–68 [CrossRef Medline](#)
9. Cairncross JG, Wang M, Jenkins RB, et al. **Benefit from procarbazine, lomustine, and vincristine in oligodendroglial tumors is associated with mutation of IDH.** *J Clin Oncol* 2014;32:783–90 [CrossRef Medline](#)
10. Choi C, Ganji SK, DeBerardinis RJ, et al. **2-hydroxyglutarate detection by magnetic resonance spectroscopy in IDH-mutated patients with gliomas.** *Nat Med* 2012;18:624–29 [CrossRef Medline](#)
11. Lin G, Chung YL. **Current opportunities and challenges of magnetic resonance spectroscopy, positron emission tomography, and mass spectrometry imaging for mapping cancer metabolism in vivo.** *Biomed Res Int* 2014;2014:625095 [CrossRef Medline](#)
12. Kumar S, Weaver VM. **Mechanics, malignancy, and metastasis: the force journey of a tumor cell.** *Cancer Metastasis Rev* 2009;28:113–27 [CrossRef Medline](#)
13. Miroshnikova YA, Mouw JK, Barnes JM, et al. **Tissue mechanics promote IDH1-dependent HIF1 $\alpha$ -tenascin C feedback to regulate glioblastoma aggression.** *Nat Cell Biol* 2016;18:1336–45 [CrossRef Medline](#)
14. Muthupillai R, Lomas DJ, Rossman PJ, et al. **Magnetic resonance elastography by direct visualization of propagating acoustic strain waves.** *Science* 1995;269:1854–57 [CrossRef Medline](#)
15. Muthupillai R, Lomas DJ, Rossman PJ, et al. **Visualizing propagating transverse mechanical waves in tissue-like media using magnetic resonance imaging.** In: Tortoli P, Masotti L, eds. *Acoustical Imaging*. Vol 22. Boston: Springer; 1996;279–83
16. Pepin KM, Ehman RL, McGee KP. **Magnetic resonance elastography (MRE) in cancer: technique, analysis, and applications.** *Prog Nucl Magn Reson Spectrosc* 2015;90–91:32–48 [CrossRef Medline](#)
17. Simon M, Guo J, Papazoglou S, et al. **Non-invasive characterization of intracranial tumors by magnetic resonance elastography.** *New J Phys* 2013;15:1–15 [CrossRef](#)
18. Reiss-Zimmermann M, Streitberger KJ, Sack I, et al. **High resolution imaging of viscoelastic properties of intracranial tumours by multi-frequency magnetic resonance elastography.** *Clin Neuroradiol* 2015;25:371–78 [CrossRef Medline](#)
19. Sakai N, Takehara Y, Yamashita S, et al. **Shear stiffness of 4 common intracranial tumors measured using MR elastography: comparison with intraoperative consistency grading.** *AJNR Am J Neuroradiol* 2016;37:1851–59 [CrossRef Medline](#)
20. Streitberger KJ, Reiss-Zimmermann M, Freimann FB, et al. **High-resolution mechanical imaging of glioblastoma by multifrequency magnetic resonance elastography.** *PLoS One* 2014;9:e110588 [CrossRef Medline](#)
21. Murphy MC, Huston J 3rd, Glaser KJ, et al. **Preoperative assessment of meningioma stiffness using magnetic resonance elastography.** *J Neurosurg* 2013;118:643–48 [CrossRef Medline](#)
22. Murphy MC, Huston J 3rd, Jack CR Jr, et al. **Measuring the characteristic topography of brain stiffness with magnetic resonance elastography.** *PLoS One* 2013;8:e81668 [CrossRef Medline](#)
23. Murphy MC, Huston J 3rd, Jack CR Jr, et al. **Decreased brain stiffness in Alzheimer's disease determined by magnetic resonance elastography.** *J Magn Reson Imaging* 2011;34:494–98 [CrossRef Medline](#)
24. Sinkus R, Tanter M, Xydeas T, et al. **Viscoelastic shear properties of in vivo breast lesions measured by MR elastography.** *Magn Reson Imaging* 2005;23:159–65 [CrossRef Medline](#)
25. Papazoglou S, Hamhaber U, Braun J, et al. **Algebraic Helmholtz inversion in planar magnetic resonance elastography.** *Phys Med Biol* 2008;53:3147–58 [CrossRef Medline](#)
26. Manduca A, Oliphant TE, Dresner MA, et al. **Magnetic resonance elastography: non-invasive mapping of tissue elasticity.** *Med Image Anal* 2001;5:237–54 [CrossRef Medline](#)
27. Clayton EH, Genin GM, Bayly PV. **Transmission, attenuation and reflection of shear waves in the human brain.** *J R Soc Interface* 2012;9:2899–910 [CrossRef Medline](#)
28. Sack I, Beierbach B, Hamhaber U, et al. **Non-invasive measurement of brain viscoelasticity using magnetic resonance elastography.** *NMR Biomed* 2008;21:265–71 [CrossRef Medline](#)
29. Jugé L, Doan BT, Seguin J, et al. **Colon tumor growth and antitumor treatment in mice: complementary assessment with MR elastography and diffusion-weighted MR imaging.** *Radiology* 2012;264:436–44 [CrossRef Medline](#)
30. Heldin CH, Rubin K, Pietras K, et al. **High interstitial fluid pressure—an obstacle in cancer therapy.** *Nat Rev Cancer* 2004;4:806–13 [CrossRef Medline](#)
31. Beiko J, Suki D, Hess KR, et al. **IDH1 mutant malignant astrocytomas are more amenable to surgical resection and have a survival benefit associated with maximal surgical resection.** *Neuro Oncol* 2014;16:81–91 [CrossRef Medline](#)